Supporting Information

Medium-temperature thermochemical energy storage based on transition metal ammoniates – a systematic comparison

Danny Müller[a,*], Christian Knoll[a,b], Georg Gravogl,[a,g] Christian Jordan[b], Elisabeth Eitenberger,[c] Gernot Friedbacher,[c] Werner Artner,[d] Jan M. Welch[e], Andreas Werner[f], Michael Harasek,[b] Ronald Miletich,[g] Peter Weinberger[a,*]

[a] Institute of Applied Synthetic Chemistry, TU Wien, Getreidemarkt 9, 1060 Vienna, Austria.

[b] Institute of Chemical, Environmental and Bioscience Engineering, TU Wien, Getreidemarkt 9, 1060 Vienna, Austria.

[c] Institute of Chemical Technologies and Analytics, TU Wien, Getreidemarkt 9, 1060 Vienna, Austria.

[d] X-Ray Center, TU Wien, Getreidemarkt 9, 1060 Vienna, Austria.

[e] Center for Labelling and Isotope Production, TRIGA Center Atominstitut, TU Wien, Stadionallee 2, 1020 Vienna, Austria.

[f] Institute for Energy Systems and Thermodynamics, TU Wien, Getreidemarkt 9, 1060 Vienna, Austria.

[g] Institut für Mineralogie und Kristallographie, University of Vienna, Althanstraße 14, 1090 Vienna, Austria

*Corresponding author danny.mueller@tuwien.ac.at
peter.e163.weinberger@tuwien.ac.at

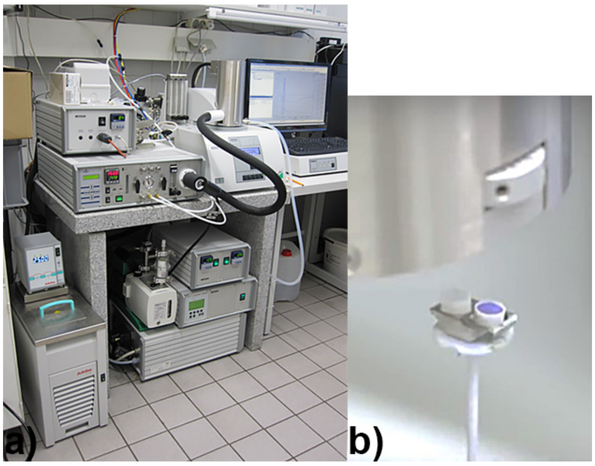

Figure S1 Used equipment for determination of the energy contents and cycle stabilities during thermal cycling under NH_3-atmosphere a) Netzsch TGA/DSC 449 C Jupiter® instrument equipped with a water vapour furnace b) Sample compartment, showing $[Ni(NH_3)_4]SO_4$ after determination of the reaction enthalpy at room-temperature (filled crucible in front) and the reference crucible (empty crucible in the back)

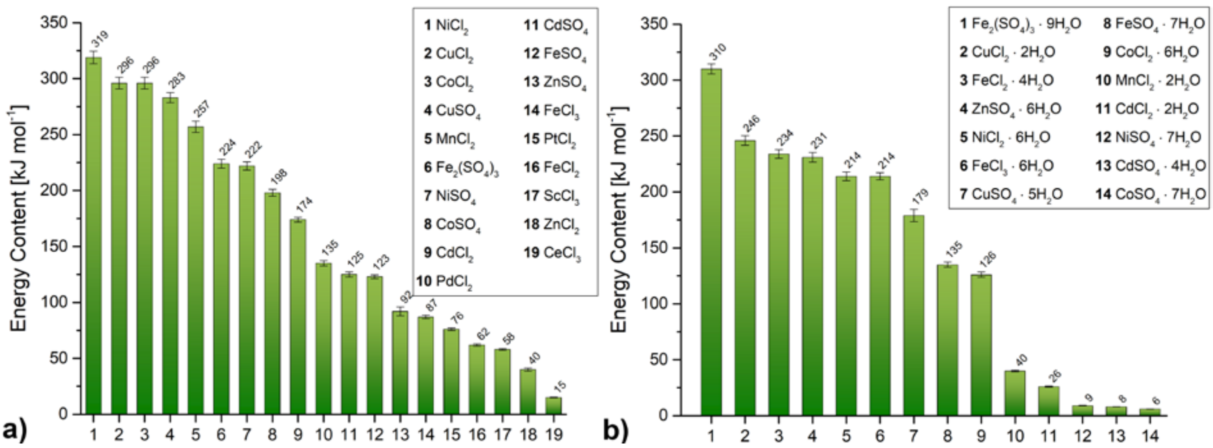

Figure S2 Energy content of selected (transition) metal salts for reaction with NH_3 at 25 °C, ranked according to the molar energy content. a) Anhydrous form of the salts b) Most common hydrate species

Table S1 Energy contents of the investigated anhydrous salts in kJ kg^{-1}, kJ mol^{-1} and energy density in MJ m^{-3} for the ammoniation reaction

Entry	Salt	kJ kg^{-1}			kJ mol^{-1}			MJ m^{-3}		
1	$NiCl_2$	2464	±	44.4	319	±	5.7	8.75	±	$1.66 \cdot 10^{-1}$
2	$CoCl_2$	2278	±	41.0	296	±	5.3	7.65	±	$1.45 \cdot 10^{-1}$
3	$CuCl_2$	2200	±	39.6	296	±	5.3	7.46	±	$1.41 \cdot 10^{-1}$
4	$MnCl_2$	2040	±	36.7	257	±	4.6	6.08	±	$1.15 \cdot 10^{-1}$
5	$CuSO_4$	1772	±	31.9	283	±	5.1	6.38	±	$1.21 \cdot 10^{-1}$
6	$NiSO_4$	1432	±	25.8	222	±	4.0	5.74	±	$1.09 \cdot 10^{-1}$
7	$CoSO_4$	1276	±	23.0	198	±	3.6	4.73	±	$8.97 \cdot 10^{-2}$
8	$CdCl_2$	947	±	17.0	174	±	3.1	3.84	±	$7.27 \cdot 10^{-2}$
9	$FeSO_4$	809	±	14.6	123	±	2.2	2.95	±	$5.60 \cdot 10^{-2}$
10	$PdCl_2$	763	±	13.7	135	±	2.4	3.05	±	$5.78 \cdot 10^{-2}$
11	$CdSO_4$	599	±	10.8	125	±	2.3	2.81	±	$5.32 \cdot 10^{-2}$
12	$ZnSO_4$	568	±	10.2	92	±	1.7	2.01	±	$3.81 \cdot 10^{-2}$
13	$Fe_2(SO_4)_3$	561	±	10.1	224	±	4.0	1.74	±	$3.30 \cdot 10^{-2}$
14	$FeCl_3$	534	±	9.6	87	±	1.6	1.55	±	$2.93 \cdot 10^{-2}$
15	$FeCl_2$	492	±	8.9	62	±	1.1	1.55	±	$2.95 \cdot 10^{-2}$
16	$ScCl_3$	386	±	6.9	58	±	1.0	0.92	±	$1.75 \cdot 10^{-2}$
17	$ZnCl_2$	291	±	5.2	40	±	0.7	0.85	±	$1.60 \cdot 10^{-2}$
18	$PtCl_2$	284	±	5.1	76	±	1.4	1.72	±	$3.26 \cdot 10^{-2}$
19	$CeCl_3$	59	±	1.1	15	±	0.3	0.23	±	$4.44 \cdot 10^{-3}$

Table S2 Energy contents of the investigated salt hydrates in kJ kg^{-1}, kJ mol^{-1} and energy density in MJ m^{-3} for the ammoniation reaction

Entry	Salt	kJ kg^{-1}			kJ mol^{-1}			MJ m^{-3}		
1	$CuCl_2 \cdot 2H_2O$	1441	±	25.9	246	±	4.4	3.66	±	$6.59 \cdot 10^{-2}$
2	$FeCl_2 \cdot 4H_2O$	1176	±	21.2	234	±	4.2	2.27	±	$4.09 \cdot 10^{-2}$
3	$NiCl_2 \cdot 6H_2O$	901	±	16.2	214	±	3.9	1.73	±	$3.11 \cdot 10^{-2}$
4	$ZnSO_4 \cdot 6H_2O$	802	±	14.4	231	±	4.2	1.66	±	$2.99 \cdot 10^{-2}$
5	$FeCl_3 \cdot 6H_2O$	792	±	14.3	214	±	3.9	1.44	±	$2.59 \cdot 10^{-2}$
6	$CuSO_4 \cdot 5H_2O$	715	±	12.9	179	±	3.2	1.64	±	$2.95 \cdot 10^{-2}$
7	$Fe_2(SO_4)_3 \cdot 9H_2O$	552	±	9.9	310	±	5.6	1.05	±	$1.89 \cdot 10^{-2}$
8	$CoCl_2 \cdot 6H_2O$	532	±	9.6	126	±	2.3	1.02	±	$1.84 \cdot 10^{-2}$
9	$FeSO_4 \cdot 7H_2O$	485	±	8.7	135	±	2.4	0.92	±	$1.66 \cdot 10^{-2}$
10	$MnCl_2 \cdot 2H_2O$	202	±	3.6	40	±	0.7	0.41	±	$7.31 \cdot 10^{-3}$
11	$CdCl_2 \cdot 2H_2O$	128	±	2.3	28	±	0.5	0.43	±	$7.67 \cdot 10^{-3}$
12	$NiSO_4 \cdot 7H_2O$	35	±	0.6	9	±	0.2	0.07	±	$1.23 \cdot 10^{-3}$
13	$CdSO_4 \cdot 4H_2O$	27	±	0.5	8	±	0.1	0.08	±	$1.5 \cdot 10^{-3}$
14	$CoSO_4 \cdot 7H_2O$	23	±	0.4	6	±	0.1	0.04	±	$8.07 \cdot 10^{-4}$

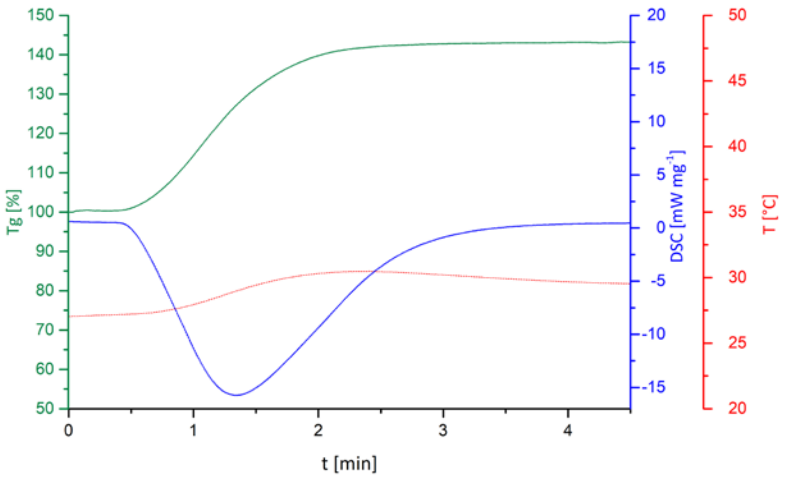

Figure S3 TGA/DSC curve for the reaction $CuSO_4$ + 4 NH_3 ↔ $[Cu(NH_3)_4]SO_4$ to determine the energy content, displayed in figure 2. The mass increase of 43 % corresponds perfectly to the expected one, going along with a full uptake of 4 NH_3 ligands.

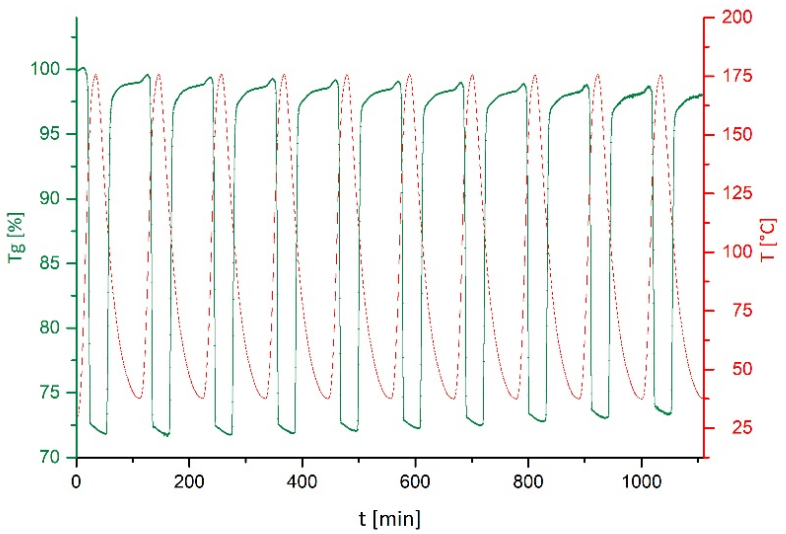

Figure S4 Cycle stability experiment of the reaction couple $[Co(NH_3)_4]Cl_2 \rightleftharpoons CoCl_2$ under NH_3 atmosphere. Mass-loss during 10 consecutive cycles: 2.1 %

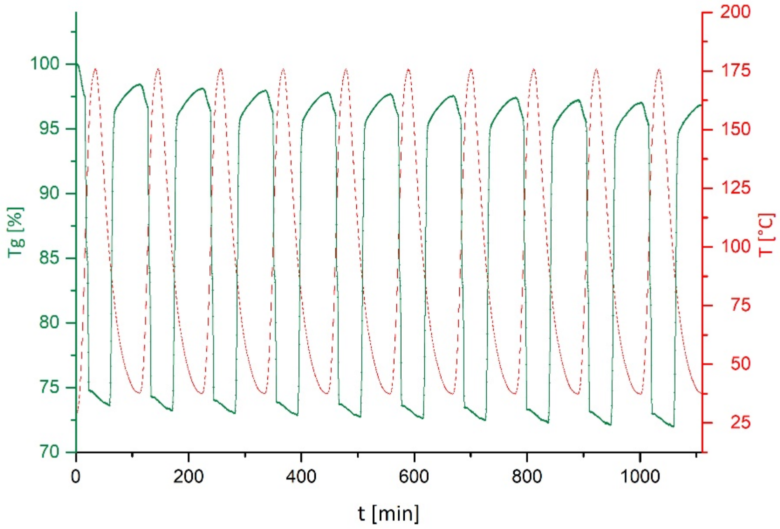

Figure S5 Cycle stability experiment of the reaction couple $[Cu(NH_3)_6]Cl_2 \rightleftharpoons CuCl_2$ under NH_3 atmosphere. Mass-loss during 10 consecutive cycles: 3.2 %

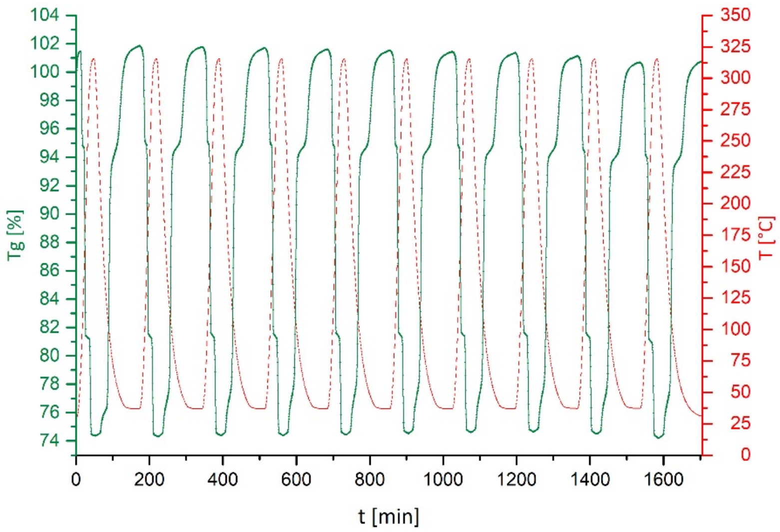

Figure S6 Cycle stability experiment of the reaction couple $[Cu(NH_3)_4]SO_4 \rightleftharpoons CuSO_4$ under NH_3 atmosphere

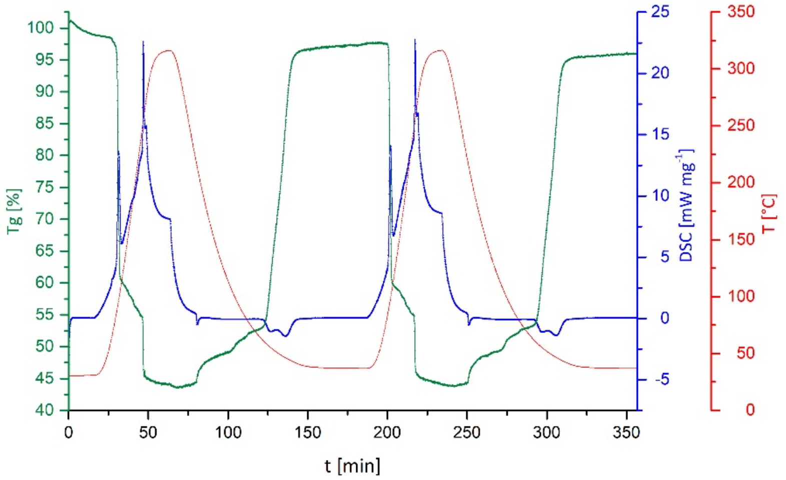

Figure S7 Two consecutive charging / discharging cycles under NH_3 atmosphere of the reaction couple $[Mn(NH_3)_2]Cl_2 \rightleftharpoons MnCl_2$

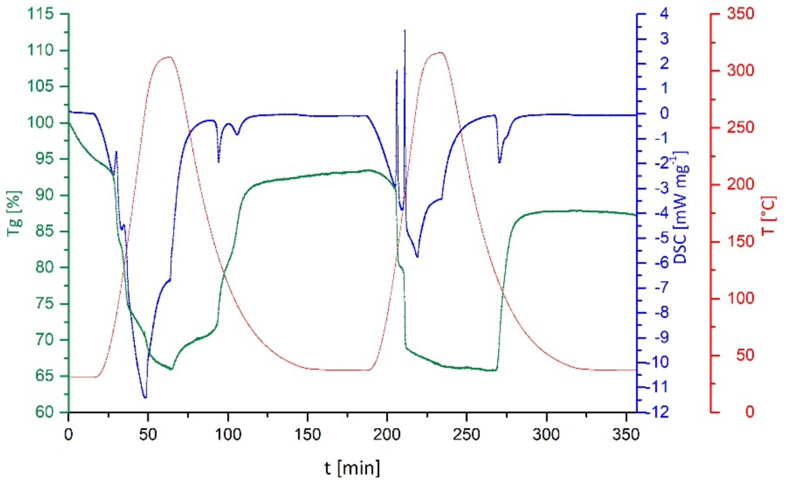

Figure S8 Two consecutive charging / discharging cycles under NH_3 atmosphere of the reaction couple $[Ni(NH_3)_4]SO_4 \rightleftharpoons NiSO_4$

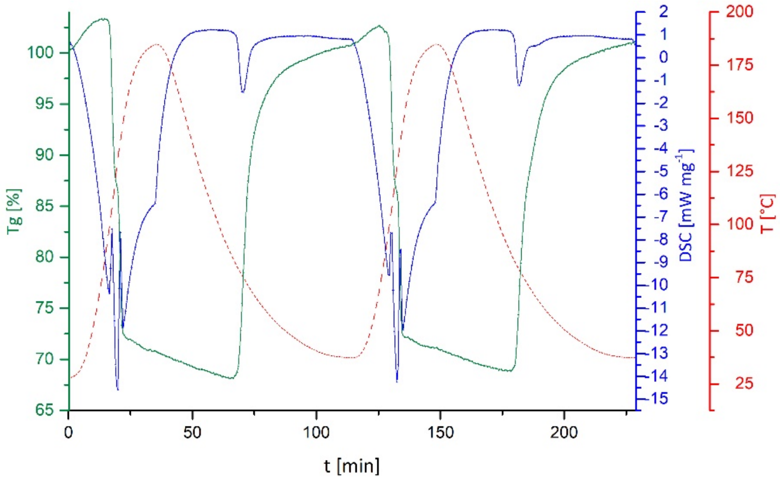

Figure S9 Two consecutive charging / discharging cycles under NH_3 atmosphere of the reaction couple $[Co(NH_3)_4]SO_4 \rightleftharpoons CoSO_4$

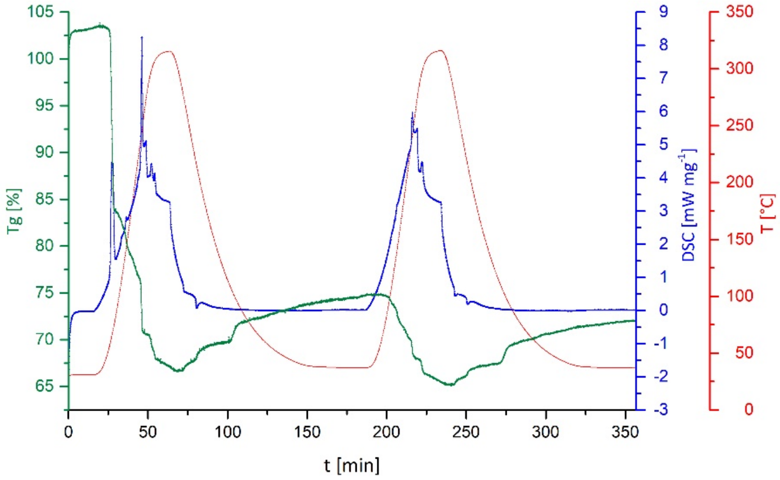

Figure S10 Two consecutive charging / discharging cycles under NH_3 atmosphere of the reaction couple $[Cd(NH_3)_4]Cl_2 \rightleftharpoons CdCl_2$

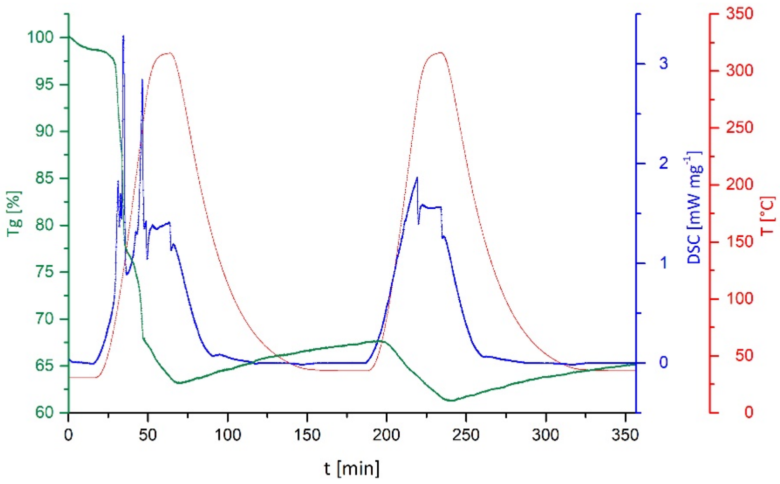

Figure S11 Two consecutive charging / discharging cycles under NH_3 atmosphere of the reaction couple $[Fe(NH_3)_2]SO_4 \rightleftharpoons FeSO_4$

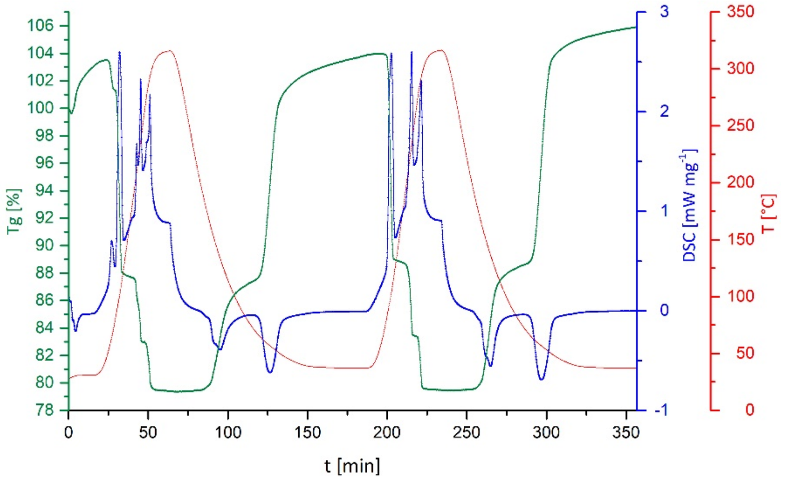

Figure S2 Two consecutive charging / discharging cycles under NH_3 atmosphere of the reaction couple $[Cd(NH_3)_2]SO_4 \rightleftharpoons CdSO_4$

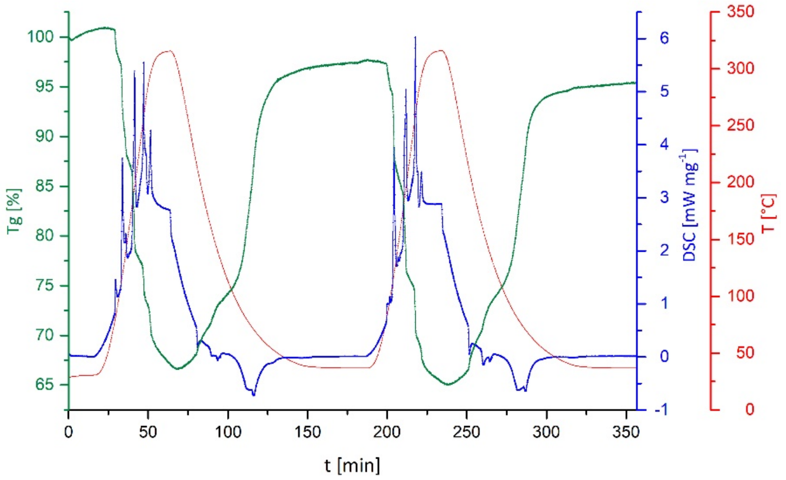

Figure S3 Two consecutive charging / discharging cycles under NH_3 atmosphere of the reaction couple $[Zn(NH_3)_4]SO_4 \rightleftharpoons ZnSO_4$

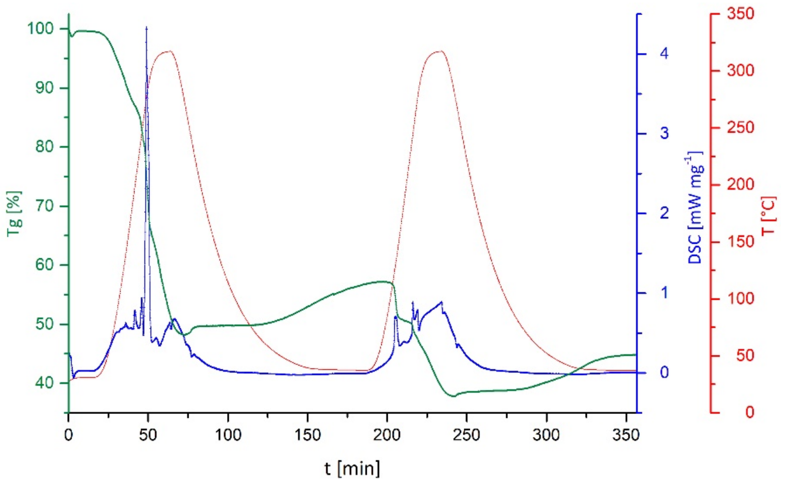

Figure S4 Two consecutive charging / discharging cycles under NH_3 atmosphere of the reaction couple $[Fe(NH_3)_3]Cl_3 \rightleftharpoons FeCl_3$

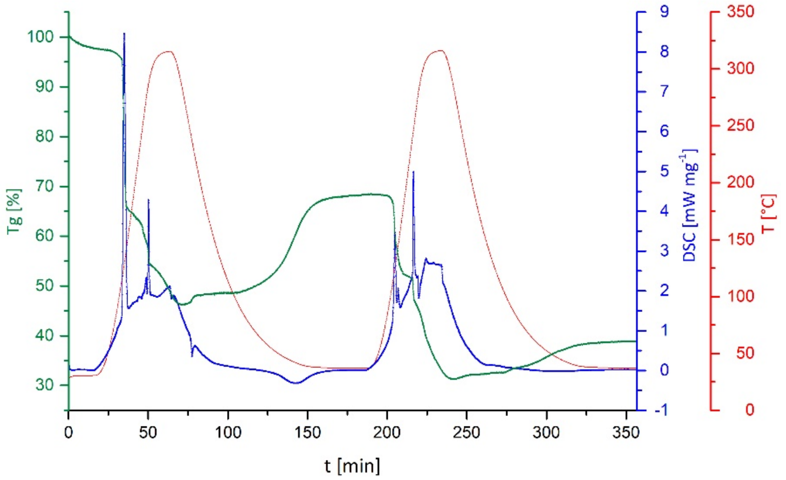

Figure S5 Two consecutive charging / discharging cycles under NH_3 atmosphere of the reaction couple $[Fe(NH_3)_3]Cl_2 \rightleftharpoons FeCl_2$

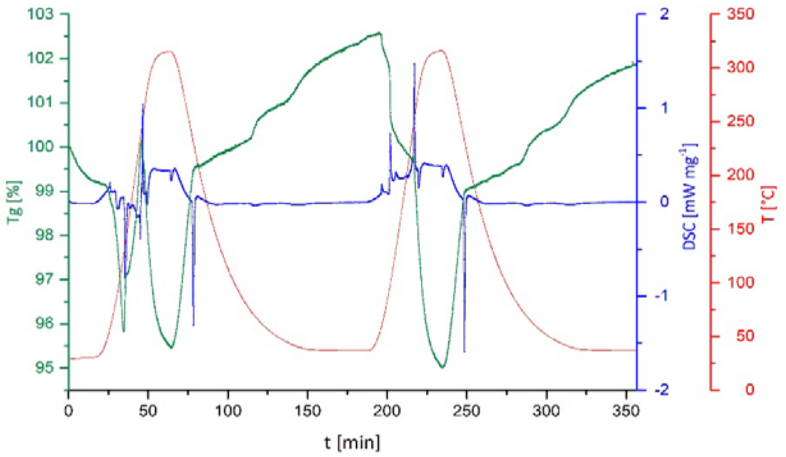

Figure S6 Two consecutive charging / discharging cycles under NH_3 atmosphere of the reaction couple $[Zn(NH_3)_4]Cl_2 \rightleftharpoons ZnCl_2$

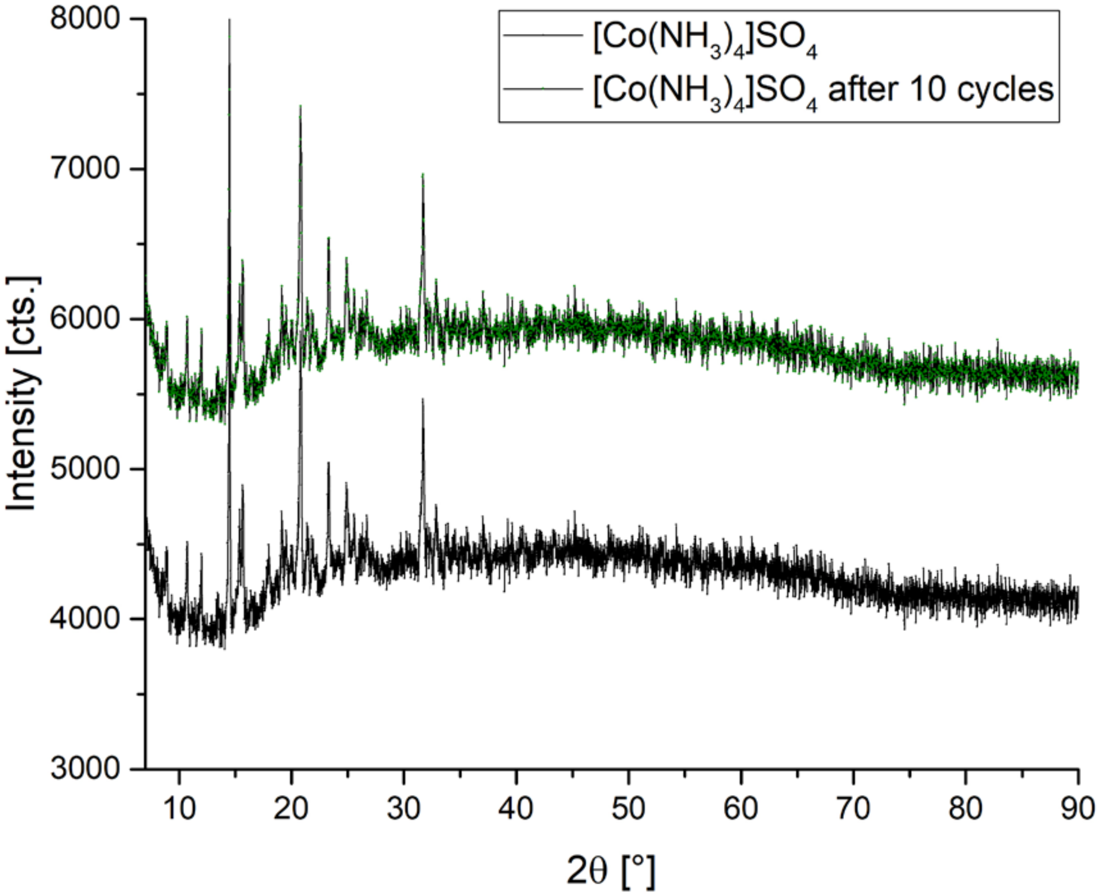

Figure S77 P-XRD of $[Co(NH_3)_4]SO_4$ before (black) and after (green) 10 heating / cooling cycles under NH_3 atmosphere

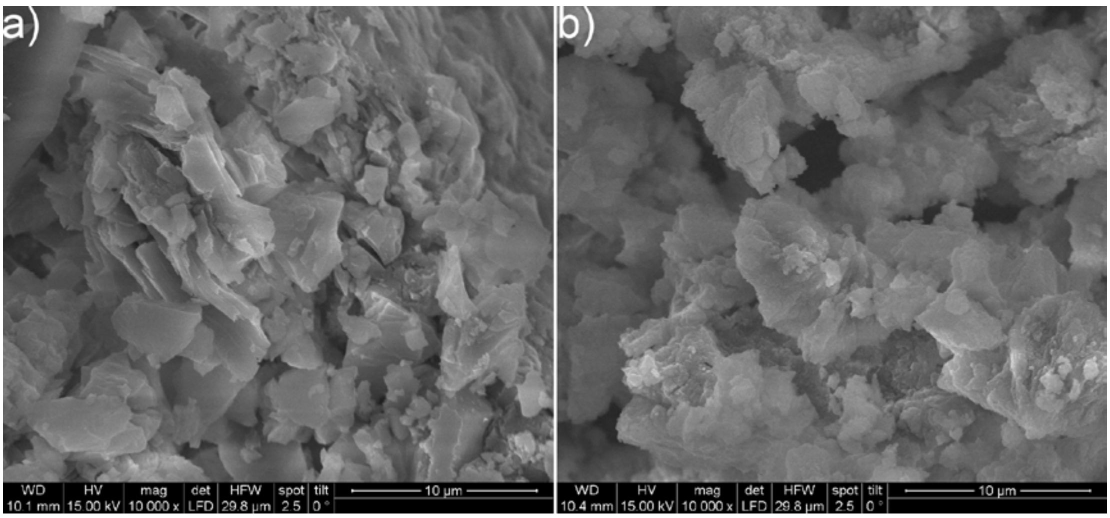

Figure S18 SEM image of $[Co(NH_3)_4]SO_4$ before (a) and after (b) 10 heating / cooling cycles under NH_3 atmosphere

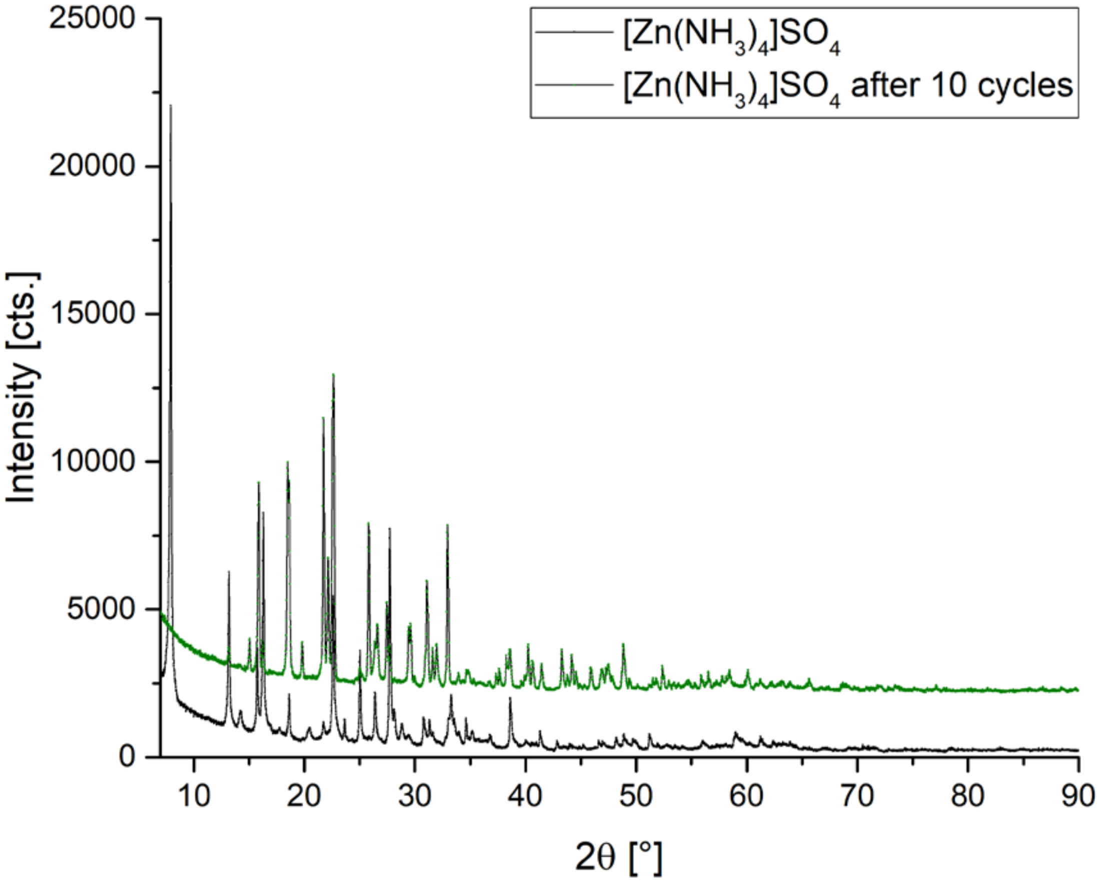

Figure S19 P-XRD of $[Zn(NH_3)_4]SO_4$ before (black) and after (green) 10 heating / cooling cycles under NH_3 atmosphere

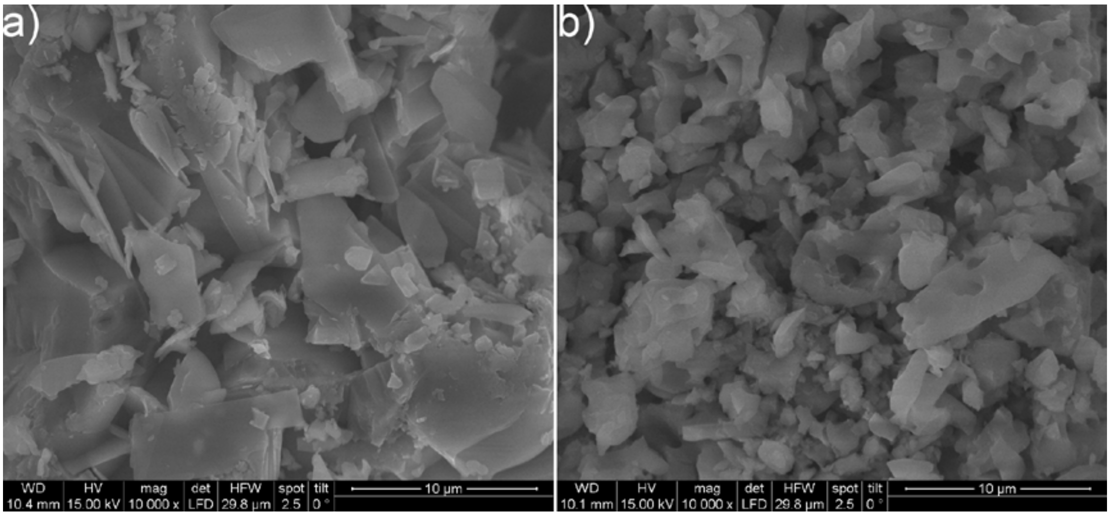

Figure S20 SEM image of $[Zn(NH_3)_4]SO_4$ before (a) and after (b) 10 heating / cooling cycles under NH_3 atmosphere

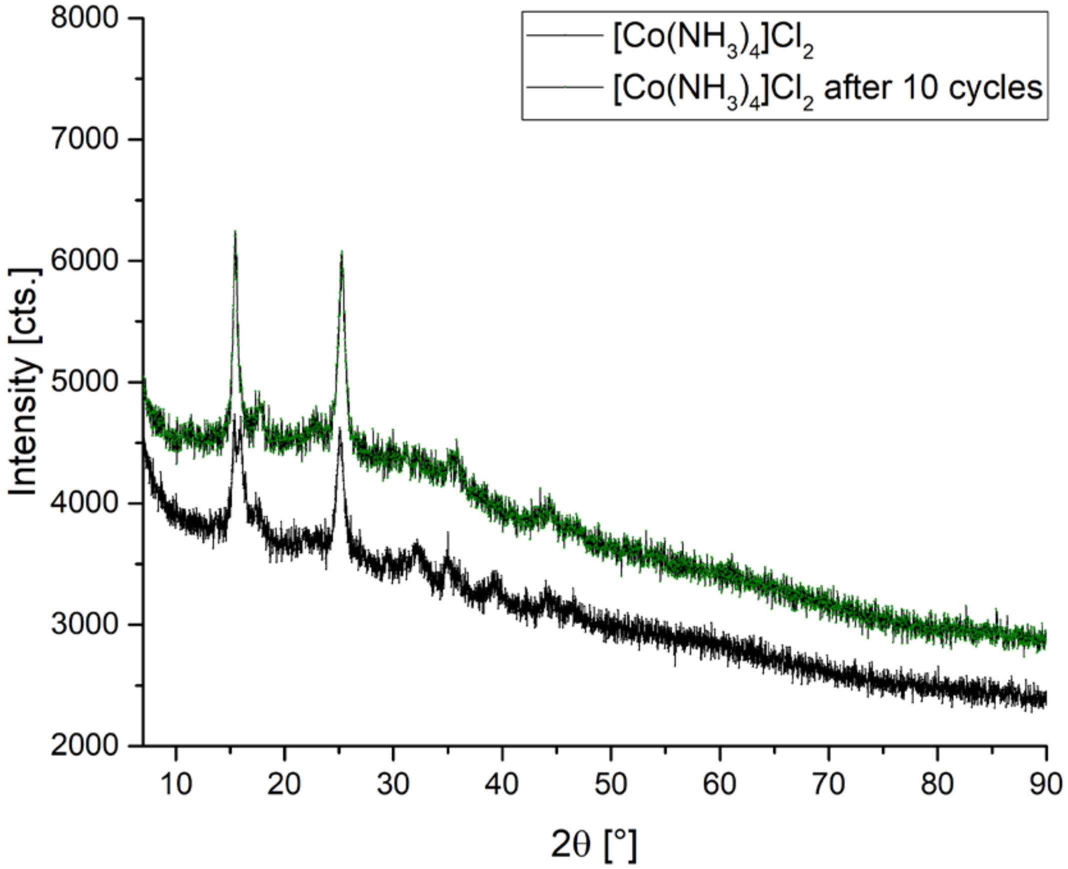

Figure S21 P-XRD of $[Co(NH_3)_4]Cl_2$ before (black) and after (green) 10 heating / cooling cycles under NH_3 atmosphere

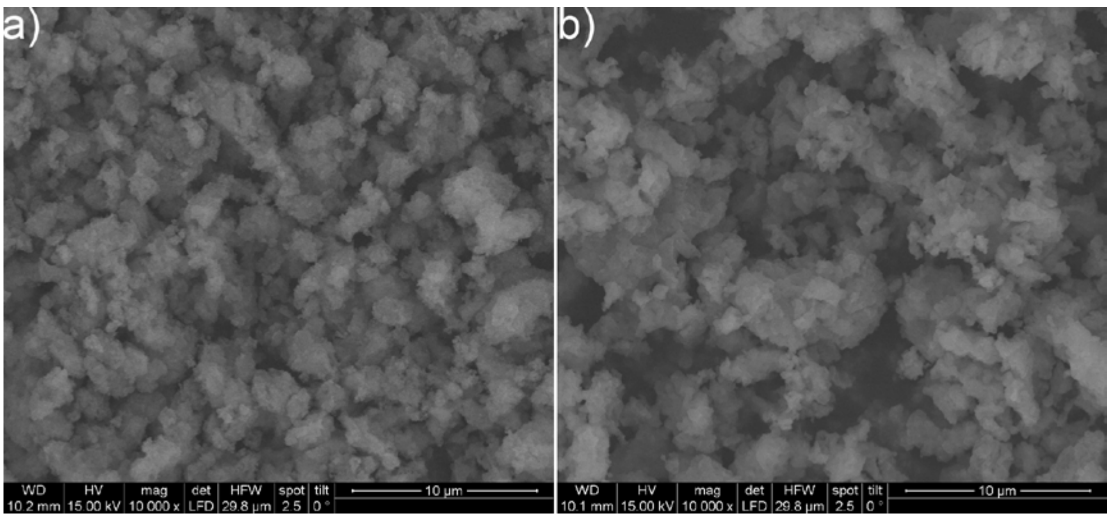

Figure S22 SEM image of $[Co(NH_3)_4]Cl_2$ before (a) and after (b) 10 heating / cooling cycles under NH_3 atmosphere

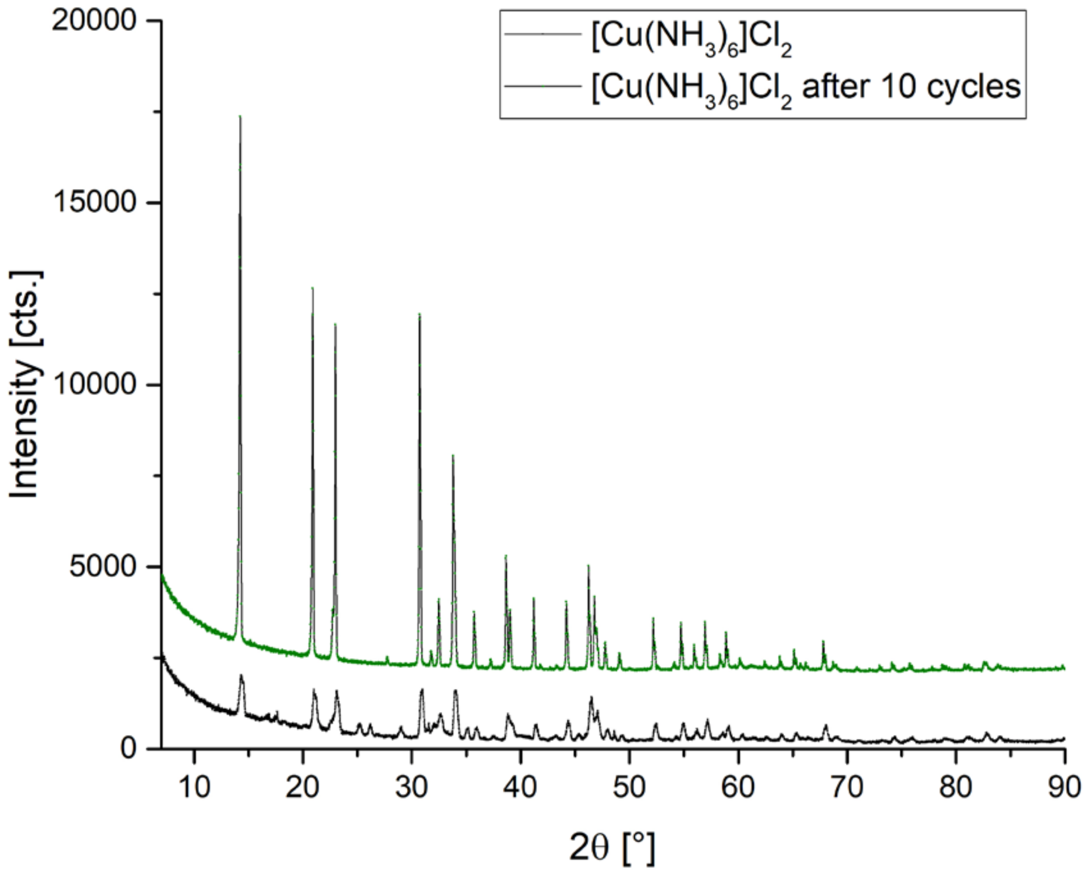

Figure S23 P-XRD of $[Cu(NH_3)_6]Cl_2$ before (black) and after (green) 10 heating / cooling cycles under NH_3 atmosphere

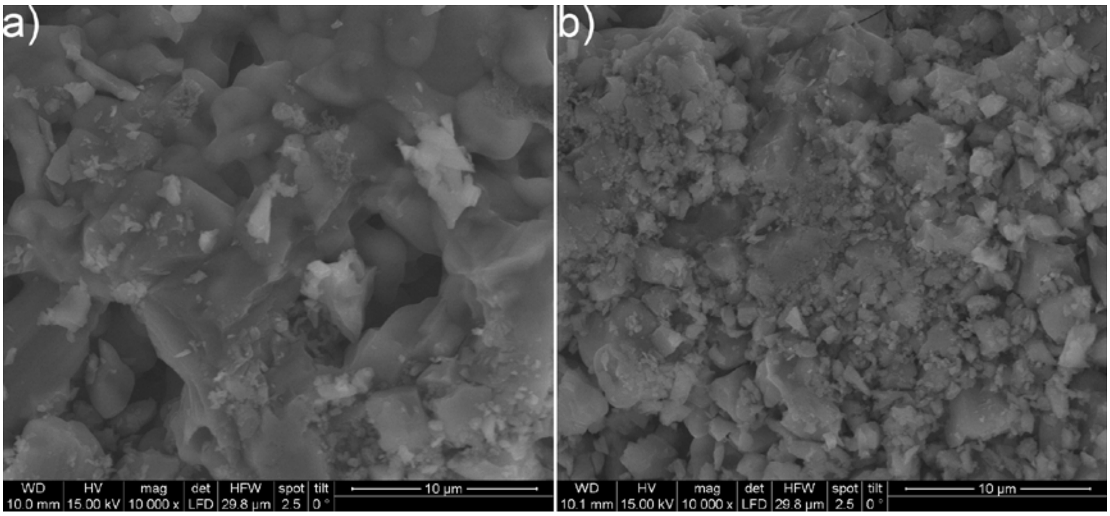

Figure S24 SEM image of $[Cu(NH_3)_6]Cl_2$ before (a) and after (b) 10 heating / cooling cycles under NH_3 atmosphere